Summer 6-24-2014

Numerical simulation of pressure pulse decay experiment on crushed low permeability rocks considering Klinkenberg effect and gas absorption/desorption

Bo Zhou
Tsinghua University

Rui-Na Xu
Tsinghua University

Pei-Xue Jiang
Tsinghua University

Proceedings of the 5th International Conference on Porous Media and its Applications in Science and Engineering
ICPM5
June 22-27, 2014, Kona, Hawaii

NUMERICAL SIMULATION OF PRESSURE PULSE DECAY EXPERIMENT ON CRUSHED LOW PERMEABILITY SHALE CONSIDERING GAS ADSORPTION/DESORPTION AND THE KLINKENBERG EFFECT

Bo Zhou, Rui-Na Xu, Pei-Xue Jiang
Thermal Science and Power Engineering Key Laboratory of Ministry of Education,
Beijing Key Laboratory of CO2 Utilization and Reduction Technology,
Department of Thermal Engineering, Tsinghua University, Beijing, China

ABSTRACT
Pressure pulse decay method is widely used for permeability tests for low permeability rock plug samples. This method can be used for crushed grain samples by removing the downstream chamber in standard pulse decay tests. Processes in pulse decay tests for low permeability crushed shale are investigated using numerical simulation. Both the Klinkenberg slip effect for gas flows in low permeability rock and the gas absorption/desorption in the porous matrix are considered. The complete mathematical model is set up to include the two effects. Deviation of the numerical pulse decay curve from the analytical one with an assumption that the pressure keeps a constant in the porous sample is investigated. The relative importance of gas absorption/desorption and gas compressibility is also investigated quantitatively. According to the present investigation, gas compressibility and adsorption both make negative contributions to the permeating process. A potential two-curve method is proposed to decide absolute permeability and the Klinkenberg coefficient when these two parameters cannot be distinguished using one pulse decay curve during the inverse fitting procedure. These two parameters can be determined at the same time only if the experiment is conducted under big initial pressure difference and the Klinkenberg coefficient has at least the same order of magnitude as the pressure.

INTRODUCTION
Gas-bearing shale is a kind of porous media with ultra-low permeability, whose information such as porosity and permeability are very important in shale gas production industry. The pore size for shale matrix ranges in 1 nm and 100 nm[12], which causes non-Darcy flows in natural gas exploiting processes and laboratory permeability tests [4,7]. When gas flowing through a porous medium with nano-scale pore size, the velocity slip at the gas-solid interface becomes significant, which result in the Klinkenberg effect for marco-scale porous medium flow[7, 10]. The Klinkenberg relation treats the effective permeability as a function of local gas pressure:

$$k = k_0\left(1+\frac{b_K}{p}\right) \tag{1}$$

where k_0 is the absolute permeability and b_K is the Klinkenberg slip constant. Florence has pointed out the inner relation between this formula and rarefied gas flows in nano-scale channels [7]. The two parameters k_0 and b_K are usually decided by experiments.
Another effect must be considered when modelling flows in shale is adsorption/desorption [2, 3]. Kerogen is an important component of gas-shale, which provides a very high internal surface area to reserve natural gas. The amount of gas adsorbed at the kerogen surface changes dynamically as the pore pressure changes. A Langmuir type isothermal equation is usually used to describe gas adsorption in shale:

$$q_a = \frac{q_L p}{p_L + p} \tag{2}$$

where q_a (std m^3/kg) is the standard volume of gas adsorbed per solid mass, q_L (std m^3/kg) is the Langmuir gas volume, p_L is the Langmuir pressure (Pa).
Pressure pulse decay method is s standard technique to measure the permeability for porous media with ultra-low permeability, typically in the range of 10^{-9} D [1, 3]. The conventional steady state method which measures the pressure drop and the flow rate when a test fluid flow through a porous medium sample does not work for ultra-low porous media because the flow rate are too low to measure accurately. In a pressure pulse decay experiment, only pressure (or pressure difference) decay

curve is to be recorded while the test time is relatively short [9, 14]. The standard sample in rock analysis is cylinder shape plug sample. Gas plug samples can be viewed as one-dimensional, i.e. along the axis direction in pressure pulse decay experiments. Substitute samples are crushed quasi-spherical samples, which are easier to acquired and the corresponding apparatus is also simpler than that for plug samples [5, 13].

The apparatus for crushed porous samples are shown in figure 1. The system contains two vessels, a buffer vessel and an experimental vessel which contains spherical samples (all with radius r_0). First, let the gas fill the buffer vessel and maintain a relatively high pressure. Second, let the high pressure gas crushed into the experimental vessel which is at pressure p_{1i} and then turn off the valve (a preheat process may be needed if the Joule-Thompson effect is significant). At this instant, the buffer vessel and the void volume V_0 of the experimental vessel both have pressure p_{0i} when equilibrium is reached. Then the gas in the volume V_0 begins to permeate in the low permeability samples along the radius direction slowly until the pressure in the void volume and the pore space becomes equilibrium again. The pressure difference gauge records the process of pressure decay in the experimental vessel and an analysis on the curve will provide information about the porous medium.

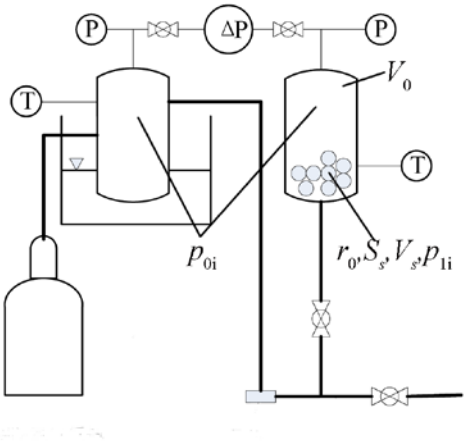

Figure 1 Apparatus for pressure pulse decay experiment for crushed spherical porous media samples with ultra-low permeability.

In the present article, we will set up the complete mathematical description of the pressure pulse decay experiment introduced above. We will compare the approximated analytical solution and the accurate numerical solution to show the importance of the gas compressibility and adsorption. Finally, an investigation on the inverse problem, i.e. the experiment data processing method, will be shown. We provide a potential solution to decide both the absolute permeability k_0 and the Klinkenberg slip constant b_K using two pressure decay curves.

NOMENCLATURE

A = the fitting constant for data processing
b_K = the Klinkenberg coefficient
c_g = isothermal compressible coefficient
e = error to the estimated parameter k/ε
F = adsorption-modified geometry constant
f = geometry constant for the apparatus
k = effective permeability
k_0 = absolute permeability
M_g = gas mass (kg) per kmol
p = pressure
p_{0i} = initial pressure in void volume V_0
p_{1i} = initial pressure
p_f = steady state pressure
p_L = the Langmuir pressure
q = adsorbate density per unit sample volume
q_a = the standard volume of gas adsorbed per solid mass
q_L = the Langmuir gas volume
R = 8314kJ/(kmol·K)/M_g
r = space coordinate
r_0 = sample radius
S_s = total sample surface area
T = temperature
t = time coordinate
t_0 = characteristic time
u = the Darcy velocity
V_0 = experiment vessel void volume
V_s = total sample volume
V_{std} = ideal gas volume per kmol in standard state
z = gas compressibility factor
x = $\varepsilon_a/\varepsilon$

Greek Symbols

ε = porosity
ε_a = effective porosity caused by adsorption
μ = gas viscosity
ρ = gas density
ρ_s = solid density
φ = root of the characteristic equation

Subscripts

0 = value in the reference state for gas properties
adsor = adsorption
comp = compressibility
ref = reference
~ = non-dimensional coordinate

1 Governing equations for pressure pulse decay experiments with spherical samples

Since the gas used in the pressure pulse decay permeates in all the spherical samples along the radius direction, the governing equation is one-dimensional in space. Considering the adsorption effect, the continuity equation is:

$$\varepsilon\frac{\partial\rho}{\partial t}+(1-\varepsilon)\frac{\partial q}{\partial t}=\frac{1}{r^2}\frac{\partial}{\partial r}\left(r^2\rho u\right) \tag{3}$$

where ρ is gas density, q is adsorbate density per unit sample volume, ε is porous medium porosity, u is Darcy velocity. Apply the Darcy equation, the Langmuir isothermal and the equation of state:

$$u=-\frac{k}{\mu}\frac{\partial p}{\partial r} \tag{4}$$

$$q=\frac{\rho_s M_g q_a}{V_{std}}=\frac{\rho_s M_g}{V_{std}}\frac{q_L p}{p_L+p} \tag{5}$$

$$p=z\rho RT, c_g=\frac{1}{\rho}\left(\frac{\partial\rho}{\partial p}\right)_T \tag{6}$$

where μ is gas viscosity, c_g is isothermal compressible coefficient. Then (3) can be converted to a parabolic equation of pressure [2, 3]:

$$\frac{\partial p}{\partial t}=\frac{1}{c_g\rho(\varepsilon+\varepsilon_a)r^2}\frac{\partial}{\partial r}\left(\frac{r^2\rho k}{\mu}\frac{\partial p}{\partial r}\right) \tag{7}$$

where ε_a is a pressure dependent effective porosity caused by adsorption:

$$\varepsilon_a=(1-\varepsilon)\frac{\rho_s M_g}{V_{std}}\frac{p_L q_L}{(p_L+p)^2}\frac{1}{c_g\rho} \tag{8}$$

As the gas permeate into the samples, the gas mass in the void volume of the experimental vessel decreases. Thus the boundary condition at the surfaces of spheres is:

$$V_0\left(\frac{\partial\rho}{\partial t}\right)_{r=r_0,t}=S_s\left(-\frac{\rho k}{\mu}\frac{\partial p}{\partial r}\right)_{r=r_0,t} \tag{9}$$

Another two boundary conditions are the symmetry condition at the sphere center and a step function as initial condition:

$$\left(\frac{\partial p}{\partial t}\right)_{r=0,t}=0 \tag{10}$$

$$p(r\neq r_0,t=0)=p_{1i}, p(r=r_0,t=0)=p_{0i} \tag{11}$$

The solution of equation (7) subject to boundary conditions (9), (10) and (11) will provide the pressure data of the samples and the pressure p_0 at the sample surfaces can be measured by sensor. A fitting to curve $p_0(t)$ with the permeability as parameter provides a method to determine permeability related information, for example, k_0 and b_K.

Now set the state of which the pressure is p_{0i} and the temperature is T as a reference state. The corresponding gas properties are denoted with subscript 0. A non-dimensional time t_0 can be defined as:

$$t_0=\frac{r_0^{\,2}\varepsilon\mu_0 c_{g0}}{k_0} \tag{12}$$

Neglecting the adsorption temporally, a steady state pressure can be reached when the test time is sufficiently long. This pressure, denoting as p_f, can be calculated as:

$$p_f=\frac{\varepsilon V_s p_{1i}+V_0 p_{0i}}{\varepsilon V_s+V_0}=\frac{fp_{1i}+3p_{0i}}{f+3} \tag{13}$$

$$f=\frac{\varepsilon r_0 S_s}{V_0} \tag{14}$$

is an apparatus related geometry constant. The pressure p_0 decays from p_{0i} to p_f during the experiment (assuming no adsorption). Using t_0 and r_0 as non-dimensionalize parameter for time and space, assuming the gas is ideal furtherly (z=1, c_g=1/p, μ=μ_0), equation (7) becomes:

$$\frac{p_{0i}}{p}\frac{\partial p^2}{\partial\tilde{t}}=\frac{1}{1+\varepsilon_a/\varepsilon}\frac{\partial}{\partial\tilde{r}}\left(\tilde{r}^2\left(1+\frac{b_K}{p}\right)\frac{\partial p^2}{\partial\tilde{r}}\right) \tag{15}$$

and the boundary condition (9) now reads:

$$\frac{p_{0i}}{p}\left(\frac{\partial p^2}{\partial\tilde{t}}\right)_{r=1}=-f\left(\frac{\partial p^2}{\partial\tilde{r}}\right)_{r=1} \tag{16}$$

Equation (15) involves three effects explicitly: compressibility, adsorption and the Klinkenberg slip. If we neglect the compressibility effect, i.e. assuming the pressure in the samples keeps around a constant (p_{0i}) all the time, the non-linearity disappears and an analytical solution can be derived using the Laplace transformation method [8]. Since the pressure in the samples ranges in p_{1i} and p_{0i}, the analytical solution is reasonable only if the relative pressure difference $(p_{0i}-p_{1i})/p_{0i}$ is small.

The approximated analytical solution of equation (15) subjected to corresponding boundary conditions are:

$$p^2(\tilde{r},\tilde{t})-\left(\frac{3p_{0i}+Fp_{1i}}{3+F}\right)^2=\sum_{n=1}^{\infty}\frac{2\sin(\varphi_n\tilde{r})\exp(-\frac{1+b_K/p_{0i}}{1+x}\varphi_n^2\tilde{t})(p_{0i}^2-p_{1i}^2)}{\tilde{r}[\varphi_n\cos\varphi_n+(2+F)\sin\varphi_n]} \tag{17}$$

where φ_n is the nth root for characteristic equation:

$$\tan\varphi=\frac{F\varphi}{\varphi^2+F} \tag{18}$$

$$F=f(1+\varepsilon_a(p_{0i})/\varepsilon)\equiv f(1+x) \tag{19}$$

Solution (17) can be truncated to reserve only the first term in the summation when the non-dimensional time is sufficiently large. Figure 2 shows that when the non-dimensional time is larger than 0.2, the first root φ_1

dominates the decay. This behavior provides a fast experiment data processing method, which is called "late-time technique" in the literature [3]. This method is only reasonable if the gas compressibility can be neglected.

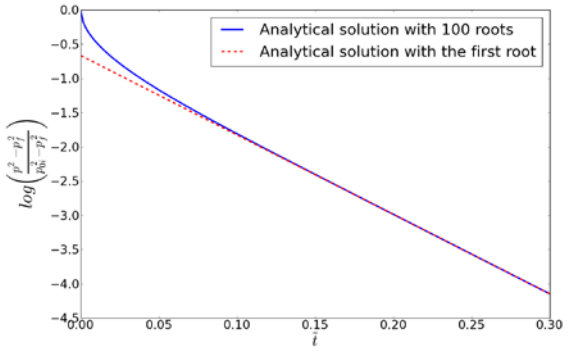

Figure 2 Analytical solutions calculated using the first 100 roots or the first root of the characteristic equation, where x=0, b_K=0, f=1, p_{0i}=10^5Pa, p_{1i}=8×10^4Pa

2 Impacts of compressibility and adsorption

In cases where the pressure drop in the samples is so large that the gas compressibility must be taken into account, equation (15) has no analytical solution. The coefficient $(1+x)^{-1}$contributed by the adsorption effect also varies as the pressure distribution changes in such cases. However, the quasi-linear equation (15) can be solved numerically using the finite difference method. Figure 3 shows numerical results with several modes. The gas used in the simulation is nitrogen. Parameters involved in the adsorption effect are p_L=7.5×10^6Pa, q_L=0.01m^3/kg, ρ_s=2500kg/m^3, V_{std}=22.414std m^3/kmol. The transport equation (15) can be written as:

$$\frac{\partial p}{\partial \tilde{t}} = \frac{1}{1+\varepsilon_a/\varepsilon}\frac{\partial}{\partial \tilde{r}}\left(\tilde{r}^2\left(\frac{p+b_K}{p_{0i}}\right)\frac{\partial p}{\partial \tilde{r}}\right) \tag{20}$$

Since p_{0i} is set as the reference state in the non-dimensionalize procedure, which is the highest pressure in the transport process, the non-dimensional transport coefficient p/p_{0i} is always less than 1 when b_K is absent. Thus the compressibility always slows down the transport process, as that is shown in figure 3. The contribution of adsorption to the transport coefficient is also negative, so the evaluation towards the equilibrium state becomes slower when adsorption is considered. Adsorption also influences the final steady state pressure since this effect contributes an effective porosity to the porous medium.

Further investigations on compressibility and adsorption respectively are shown in figure 4 and figure 5. If the late-time technique, i.e. the analytical solution, is still used to process an experiment pressure decay curve where the compressibility must be considered, an error to the parameter k_0 to be determined will occur. The

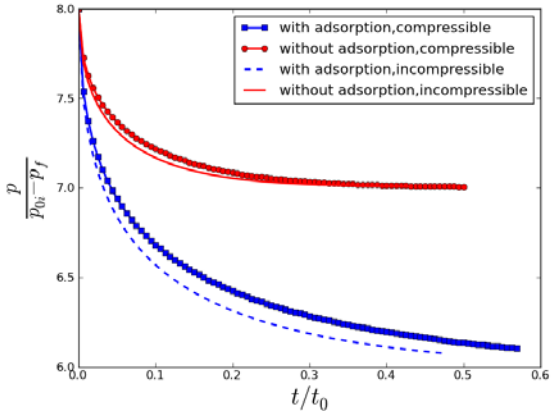

Figure 3 Numerical solutions with or without adsorption and compressibility, where b_K=0, f=1, p_{0i}=10^5Pa, p_{1i}=5×10^4Pa

dimensional form exponent in the analytical solution (the first term) gives:

$$\frac{k}{\varepsilon+\varepsilon_a} = \frac{Ar_0^{\,2}\mu_0 c_{g0}}{\varphi_1^2} \tag{21}$$

where A(s^{-1}) is a fitting parameter (assuming an exact value here). When adsorption is absent, the relative deviation of the porous medium transport parameter k/ε is:

$$e_{comp} = \frac{At_0}{\varphi_1^2} - 1 \tag{22}$$

Figure 4 shows a contour of e_{comp} as a function of geometry parameter f and the relative pressure difference $(p_{0i}-p_{1i})/p_{0i}$. As discussed above, ignoring the compressibility will underestimate the transport coefficient. The error caused by ignoring compressibility increases as the non-dimensional pressure difference increases. The geometry parameter f also influences this error because the root φ_1 is a function of f.

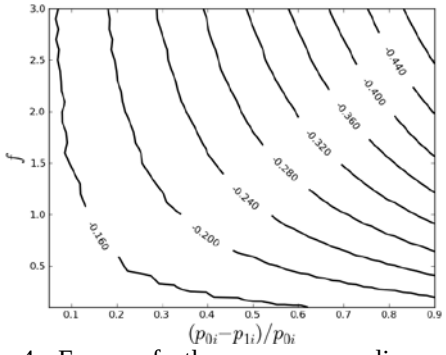

Figure 4 Error of the porous medium transport coefficient k/ε caused by ignoring compressibility

Now we investigate on the adsorption effect if the gas can be viewed as incompressible during the experiment. The model (21) is accurate in such case, the adsorption affects the characteristic root φ_1 only. The error of the transport coefficient $k/(\varepsilon+\varepsilon_a)$ is:

$$e_{adsor} = \frac{\varphi_1^2(F)}{\varphi_1^2(f)} - 1 \tag{23}$$

Figure 5 shows a contour of e_{adsor} as a function of geometry parameter f and the parameter x defined in (19). As x increases (the adsorption enhances), the error caused by ignoring adsorption increases. The geometry parameter f also influences the error.

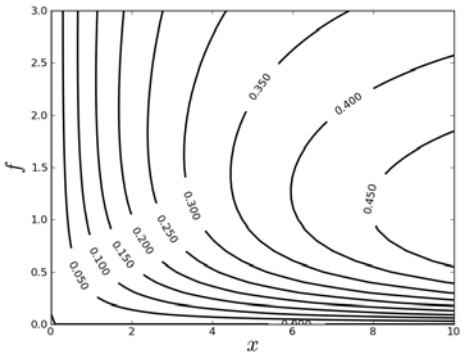

Figure 5 Error of the porous medium transport coefficient $k/(\varepsilon+\varepsilon_a)$ caused by ignoring adsorption

2 Determine the absolute permeability and the Klinkenberg coefficient by solving the inverse problem

The impact of the Klinkenberg effect to the pressure decay curve $p_0(t)$ is relatively clear. The positive constant b_K will enhance the term $(p+b_K)/p_{0i}$ and hence the effective permeability. Noticing that the absolute permeability k_0 is involved in the non-dimensional time, we conclude that in the following two cases k_0 and b_K cannot be distinguished by applying the inverse problem fitting on pressure decay curves:

1) Incompressible cases. If the pressure in the sample remains closely to p_{0i} then the term $(p+b_K)/p_{0i}$ is also nearly a constant. Only the combination $(p+b_K)k_0/p_{0i}$ (which is a constant) can be got in the inverse problem.
2) Cases where $b_K \ll p_{0i}$. In such cases it is hard to capture b_K numerically since its contribution to the pressure decay curve is covered up by the absolute permeability.

The inverse problem is solved as the following steps. First evaluate a pressure decay curve using $k_{0,ref}$ and $b_{K,ref}$, which are fitting parameters. Second choose M discrete data points as sample and define an optimization function:

$$R(k_0, b_K) = \sum_{n=1}^{M} \left(p_{0,fit,n}(k_0, b_K) - p_{0,ref,n} \right)^2 \tag{24}$$

where $p_{0,fit,n}$ is the nth data point of the curve calculated using predicting parameters k_0 and b_K, $p_{0,ref,n}$ is the nth data point of the sample set. Finally, minimize the function R subjected to positive k_0 and b_K. The algorithm using here is the Sequential Least SQuares Programming (SLSQP) Constrained minimization method [11].

Figure 6 and figure 7 show fitting result for cases $k_{0,ref}=1\times10^{-18}\text{m}^2$, $b_{K,ref}=5\times10^4\text{Pa}$ and $k_{0,ref}=1\times10^{-18}\text{m}^2$, $b_{K,ref}=1\times10^5\text{Pa}$ respectively. Other related parameters are $p_{0i}=1\times10^5\text{Pa}$, $f=1$, $x=0$. The initial values (shown as hollow squares) for the optimization procedures are randomly selected in the range an order of magnitude more or less than the reference parameters. Two sample data are evaluated using different initial pressure p_{1i} for each case.

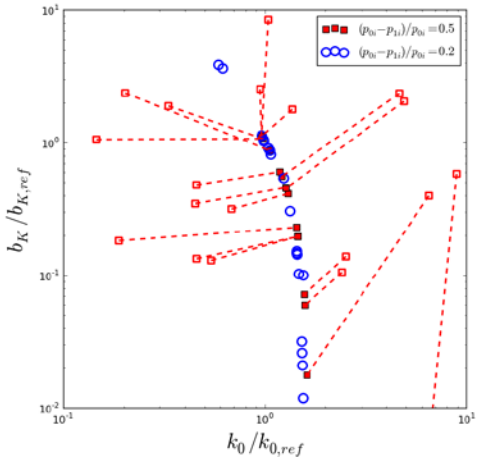

Figure 6 Inverse fitting results for case $b_{K,ref}=5\times10^4\text{Pa}$

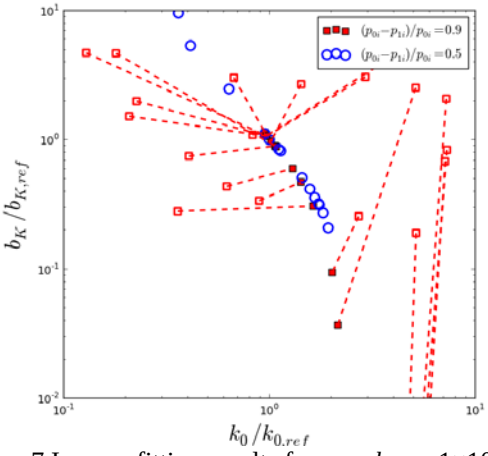

Figure 7 Inverse fitting results for case $b_{K,ref}=1\times10^5\text{Pa}$

For each case the target value of fitting is (1,1) in figure 6 and figure 7. Fitting results with different initial pressure p_{1i} and hence different pressure difference $(p_{0i}-p_{1i})/p_{0i}$ give similar curves. Parameters ($k_0/k_{0,ref}$, $b_K/$

$b_{K,ref}$) on these curves can all make calculated pressure decay curves and the sample data match. However, points satisfy both decay curves with different pressure difference concentrated near the point (1,1). When b_K is comparable to p_{0i} in order of magnitude, an intersection zone of the fitting result curves gradually forms, which also covers the desired point (1,1). This observation verifies the prior analysis in this section that we can hope to distinguish k_0 and b_K only if b_K is comparable to p_{0i} and compressibility is considered. Furthermore, two sets of sample data, i.e. two experiment pressure decay curves (with different initial pressure difference) are required at least.

A substitute way to calculate k_0 and b_K is to calculate the effective permeability at various pressure and then fit the data using the Klinkenberg relation. This method is adopted in the conventional steady state permeability test, which also works here. More experiment pressure decay curves are needed to get accurate fitting results.

CONCLUSIONS

A complete mathematical model for the pressure pulse decay experiment for crushed shale matrix samples with ultra-low permeability is built in the present article. For shale matrix, both the Klinkenberg effect and adsorption/desorption must be taken into account. After the non-dimensionalize procedure, we find that compressibility, the Klinkenberg effect and adsorption all contributes to the effective permeability. The Klinkenberg effect makes a positive contribution while the other two effects make negative contributions. Key criterions on whether these effects are important are $(p_{0i}-p_{1i})/p_{0i}$ for compressibility, x for adsorption and b_K/p_{0i} for the Klinkenberg effect. The geometry non-dimensional factor f also influences these effects.

The investigation on the inverse fitting procedure for k_0 and b_K shows these two parameters cannot be distinguished using only one set of sample data. For cases where incompressibility is assumed or b_K is too small, the effort to distinguish them will also fail. A practice shows that we can hope to determine these two parameters using two sets of sample data produced by large initial pressure difference experiment if the parameter b_K is comparable to p_{0i}.

ACKNOWLEDGEMENT

The authors would like to acknowledge support from the National Natural Science Foundation of China(No. 51376104) and the National Science Fund for Creative Research Groups of China(No. 51321002)

REFERENCES

[1] American Petroleum Institute. Recommended Practices for Core Analysis, RP 40, 2th edition [R]. Washington: API, 1998: 6(37)-6(39)

[2] Civan F, Rai CS, Sondergeld CH (2011) Shale-gas permeability and diffusivity inferred by improved formulation of relevant retention and transport mechanisms. *Transport in Porous Media*, 86(3): 925-944.

[3] Cui X, Bustin AMM, Bustin RM (2009) Measurements of gas permeability and diffusivity of tight reservoir rocks: different approaches and their applications. *Geofluids*, 9(3): 208-223.

[4] Darabi H, Ettehad A, Javadpour F, et al (2012) Gas flow in ultra-tight shale strata. *Journal of Fluid Mechanics*, 710: 641-658.

[5] Egermann P, Lenormand R, Longeron D, Zarcone C (2005) A fast and direct method of permeability measurements on drill cuttings. *Society of Petroleum Engineers Reservoir Evaluation and Engineering*, 4, 269–75.

[6] Florence, Francois Andre, et al Improved permeability prediction relations for low permeability sands. *Rocky Mountain Oil & Gas Technology Symposium*. Society of Petroleum Engineers, 2007.

[7] Freeman CM, Moridis GJ, Blasingame TA (2011) A numerical study of microscale flow behavior in tight gas and shale gas reservoir systems. *Transport in porous media*, 90(1): 253-268.

[8] Hsieh PA, Tracy JV, Neuzil CE, Bredehoeft JD, Silliman SE (1981) A transient laboratory method for determining the hydraulic properties of 'tight' rocks: I. Theory. *International Journal of Rock Mechanics and Mining Sciences*, 18, 245–52.

[9] Jones SC (1997) A technique for faster pulse-decay permeability measurements in tight rocks. *SPE formation evaluation*, 12(01): 19-26.

[10] Klinkenberg LJ (1941) The permeability of porous media to liquids and gases. *Drilling and production practice*.

[11] Kraft, D (1998) A software package for sequential quadratic programming. Tech. Rep. DFVLR-FB 88-28, DLR German Aerospace Center – Institute for Flight Mechanics, Koln, Germany.

[12] Loucks RG, et al (2009) Morphology, genesis, and distribution of nanometer-scale pores in siliceous mudstones of the Mississippian Barnett Shale. *Journal of Sedimentary Research*, 79(12): 848-861.

[13] Luffel DL, Hopkins CW, Schettler Jr PD. Matrix permeability measurement of gas productive shales. *SPE Annual Technical Conference and Exhibition*. Society of Petroleum Engineers, 1993.

[14] Yamada SE, Jones AH (1980) A review of a pulse technique for permeability measurements. *Society of Petroleum Engineers Journal*, 20(05): 357-358.